

Fractal boundaries of complex networks

This content has been downloaded from IOPscience. Please scroll down to see the full text.

2008 EPL 84 48004

(<http://iopscience.iop.org/0295-5075/84/4/48004>)

View [the table of contents for this issue](#), or go to the [journal homepage](#) for more

Download details:

IP Address: 141.211.4.224

This content was downloaded on 15/06/2015 at 14:33

Please note that [terms and conditions apply](#).

Fractal boundaries of complex networks

JIA SHAO^{1(a)}, SERGEY V. BULDYREV^{1,2}, REUVEN COHEN³, MAKSIM KITSACK¹, SHLOMO HAVLIN⁴ and H. EUGENE STANLEY¹

¹ Center for Polymer Studies and Department of Physics, Boston University - Boston, MA 02215, USA

² Department of Physics, Yeshiva University - 500 West 185th Street, New York, NY 10033, USA

³ Department of Mathematics, Bar-Ilan University - 52900 Ramat-Gan, Israel

⁴ Minerva Center and Department of Physics, Bar-Ilan University - 52900 Ramat-Gan, Israel

received 12 May 2008; accepted in final form 16 October 2008

published online 21 November 2008

PACS 89.75.Hc – Networks and genealogical trees

PACS 89.75.-k – Complex systems

PACS 64.60.aq – Networks

Abstract – We introduce the concept of the boundary of a complex network as the set of nodes at distance larger than the mean distance from a given node in the network. We study the statistical properties of the boundary nodes seen from a given node of complex networks. We find that for both Erdős-Rényi and scale-free model networks, as well as for several real networks, the boundaries have fractal properties. In particular, the number of boundaries nodes B follows a power law probability density function which scales as B^{-2} . The clusters formed by the boundary nodes seen from a given node are fractals with a fractal dimension $d_f \approx 2$. We present analytical and numerical evidences supporting these results for a broad class of networks.

Copyright © EPLA, 2008

Many complex networks are “small world” due to the very small average distance d between two randomly chosen nodes. Often $d \sim \ln N$, where N is the number of nodes [1–6]. Thus, starting from a randomly chosen node following the shortest path, one can reach any other node in a very small number of steps. This phenomenon is called “six degrees of separation” in social networks [4]. That is, for most pairs of randomly chosen people, the shortest “distance” between them is not more than six. Many random network models, such as Erdős-Rényi network (ER) [1], Watts-Strogatz network (WS) [5] and scale-free network (SF) [3,6–8], as well as many real networks, have been shown to possess this small-world property.

Much attention has been devoted to the structural properties of networks within the average distance d from a given node. However, almost no attention has been given to nodes which are at distances greater than d from a given node. We define these nodes as the boundaries of the network and study the ensemble of boundaries formed by all possible starting nodes. An interesting question is: how many “friends of friends of friends etc. . .” has one at a distance greater than the average distance d ? What is their probability distribution and what is the structure of the boundaries? The boundaries have an important

role in several scenarios, such as in the spread of viruses or information in a human social network. If the virus (information) spreads from one node to all its nearest neighbors, and from them to all next nearest neighbors and further on until d , how many nodes do *not* get the virus (information), and what is their distribution with respect to the origin of the infection?

In this letter, we find theoretically and numerically that the nodes at the boundaries, which are of order N , exhibit similar fractal features for many types of networks, including ER and SF models as well as several real networks. Song *et al.* [9] found that some networks have fractal properties while others do not. Properties of fractal networks were also studied [10,11]. Here we show that almost all model and real networks including non-fractal networks have fractal features at their boundaries.

Figure 1 demonstrates our approach and analysis. For each “root” node, we call the nodes at distance ℓ from it “nodes in shell ℓ ”. We choose a random root node and count the number of nodes B_ℓ at shell ℓ . We see that $B_1 = 10$, $B_2 = 11$, $B_3 = 13$, etc. . . . We estimate the average distance (diameter) $d \approx 2.9$ by averaging the distances between all pairs of nodes. After removing nodes with $\ell < d \approx 2.9$, the network is fragmented into 12 clusters, with sizes $s_3 = \{1, 1, 2, 5, 1, 3, 1, 1, 8, 1, 2, 3\}$. Note that the

^(a)E-mail: jiashao@buphy.bu.edu

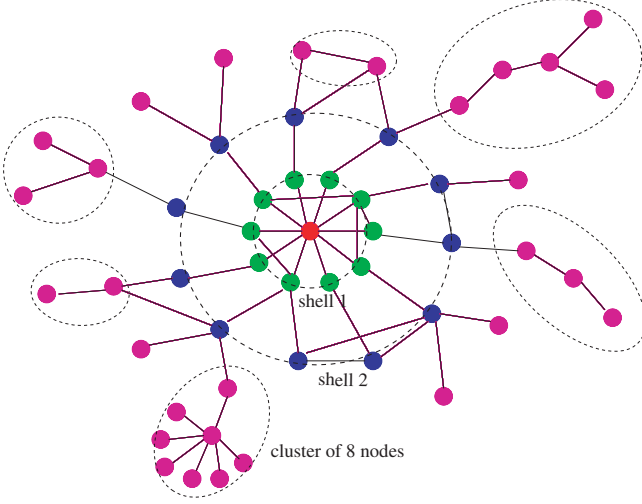


Fig. 1: (Color online) Illustration of shells and clusters originating from a randomly chosen root node, which is shown in the center (red). Its neighboring nodes are defined as shell 1 (green), the nodes at distance ℓ are defined as shell ℓ . When removing all nodes with $\ell < 3$, the remaining network (purple) becomes fragmented into 12 clusters.

boundary of the network is always seen from a given node, thus not a unique set of nodes in the network.

We begin by simulating ER and SF networks, and then we present analytical proofs. Figure 2a shows simulation results for the number of nodes B_ℓ reached from a randomly chosen origin node for an ER network. The results shown are for a single network realization of size $N = 10^6$, with average degree $\langle k \rangle = 6$ and $d \approx 7.9$ (see footnote ¹). For $\ell < d$, the cumulative distribution function, $P(B_\ell)$, which is the probability that shell ℓ has more than B_ℓ nodes, decays exponentially for $B_\ell > B_\ell^*$, where B_ℓ^* is the maximum typical size of shell ℓ (see footnote ²). However, for $\ell > d$, we observe a clear transition to a power law decay behavior, where $P(B_\ell) \sim B_\ell^{-\beta}$, with $\beta \approx 1$ and the pdf of B_ℓ is $\tilde{P}(B_\ell) \equiv dP(B_\ell)/dB_\ell \sim B_\ell^{-2}$. For different networks, the emergence of the power law can occur at shell $\ell = d + 1$ or $\ell = d + 2$. Thus, our results suggest a broad “scale-free” distribution for the number of nodes at distances larger than d . This power law behavior demonstrates that there is no characteristic size and a broad range of sizes can appear in a shell at the boundaries.

In SF networks, the degrees of the nodes, k , follow a power law distribution function $q(k) \sim k^{-\lambda}$, where the minimum degree of the network, k_{\min} , is chosen to be 2.

Figure 2b shows, for SF networks with $\lambda = 2.5$, similar power law results, $P(B_\ell) \sim B_\ell^{-\beta}$, with $\beta \approx 1$ for $\ell > d$

¹Different realizations yield similar results. In one realization, a certain fraction of nodes are randomly taken to be origin. The histogram is obtained from B_ℓ belonging to different origin nodes.

²The behavior of the pdf of B_ℓ for $\ell < d$ will be discussed later and is shown in fig. 3c.

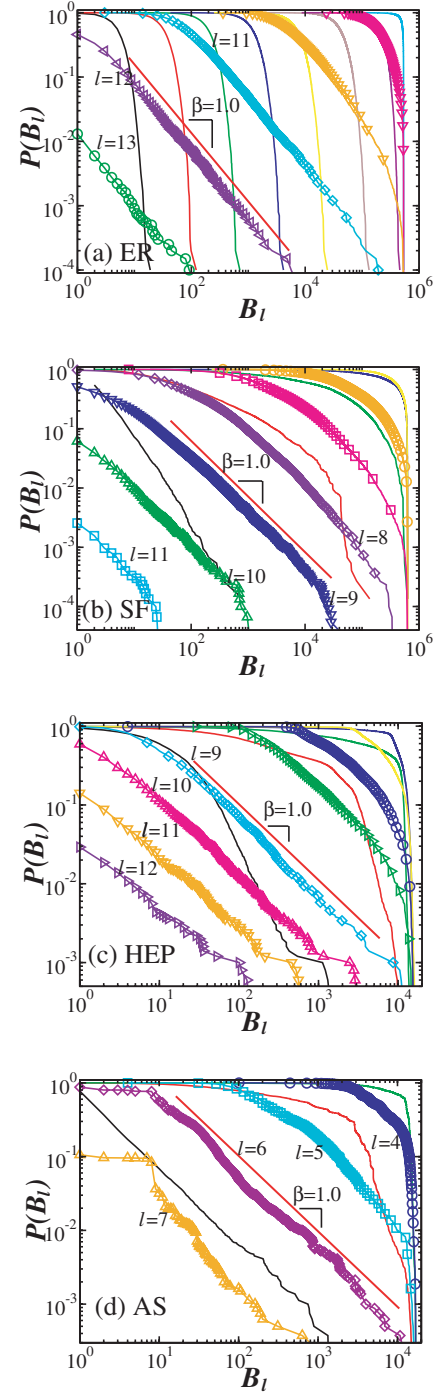


Fig. 2: (Color online) The cumulative distribution function, $P(B_\ell)$, for two random network models: (a) ER network with $N = 10^6$ nodes and $\langle k \rangle = 6$, and (b) SF network with $N = 10^6$ nodes and $\lambda = 2.5$, and two real networks: (c) the High Energy Particle (HEP) physics citations network and (d) the Autonomous System (AS) Internet network. The shells with $\ell > d$ are marked with their shell number. The thin lines from left to right represent shells $\ell = 1, 2, \dots$, respectively, with $\ell < d$. For $\ell > d$, $P(B_\ell)$ follows a power law distribution $P(B_\ell) \sim B_\ell^{-\beta}$, with $\beta \approx 1$ (corresponding to $\tilde{P}(B_\ell) \sim B_\ell^{-2}$ for the pdf). The appearance of a power law decay only happens for ℓ larger than $d \approx 7.9$ for ER and $d \approx 4.7$ for the SF network. The straight lines possess slopes of -1 .

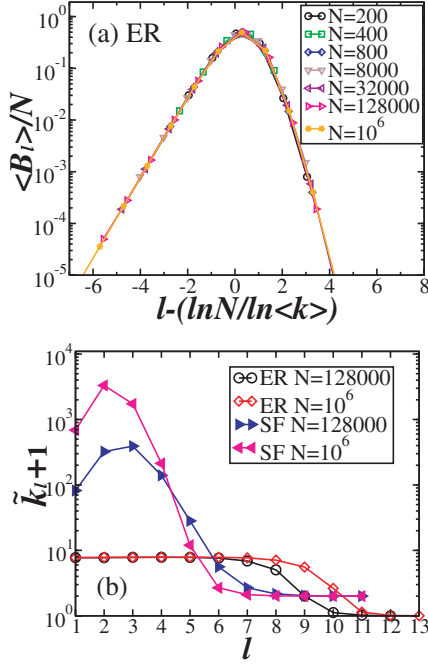


Fig. 3: (Color online) (a) Normalized average number of nodes at shell l , $\langle B_l \rangle / N$, as a function of $l - \ln N / \ln \langle k \rangle$ for ER network with $\langle k \rangle = 6$. For different N , the curves collapse. (b) $\tilde{k}_l + 1$, which is $\langle k_l^2 \rangle / \langle k_l \rangle$, as a function of l shown for both ER and SF networks with different N .

which is similar with ER. We find similar results also for $\lambda > 3$ (not shown).

To test how general is our finding, we also study several real networks (figs. 2c, d), including the High Energy Particle (HEP) physics citations network [12] and the Autonomous System (AS) Internet network [13,14]. For HEP network and AS network, $d \approx 4.2$ and 3.3 , respectively. The degree distribution of HEP network is not a power law (see fig. 2c), while the AS network shows a power law degree distribution with $\lambda \approx 2.1$ (see fig. 2d). Our results suggest that the power law decay behavior appears also in both networks, with similar values of $\beta \approx 1$ for $l > d$ (see footnote ³).

Next we ask: how many nodes are on average at the boundaries? Are they a nonzero fraction of N ? We calculate the mean number $\langle B_l \rangle$ in shell l , and in fig. 3a plot $\langle B_l \rangle / N$ as a function of $l - \ln N / \ln \langle k \rangle$ for different values of N for ER network. The term $\ln N / \ln \langle k \rangle$ represents the diameter d of the network [2]. We find that, for different values of N , the curves collapse, supporting a relation independent of network size N . Since $\langle B_l \rangle / N$ is apparently constant and independent of N , it follows that $\langle B_l \rangle \sim N$, *i.e.*, a finite fraction of N nodes appears at each shell including shells with $l > d$. We find similar behavior for SF network with $\lambda = 3.5$ (not shown).

³We also find similar results (not shown here) for other real networks.

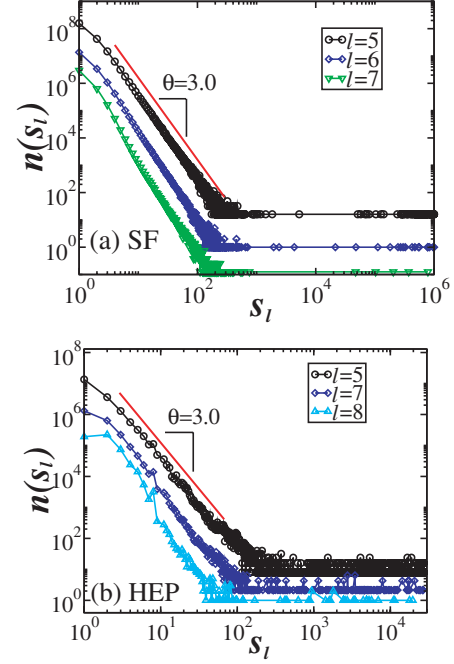


Fig. 4: (Color online) The number of clusters of sizes s_l , $n(s_l)$, as a function of s_l after removing nodes within shell l for: (a) SF network with $N = 10^6$ and $\lambda = 2.5$, (b) HEP citations network. The relation between $n(s_l)$ and s_l is characterized by a power law, $n(s_l) \sim s_l^{-\theta}$, with $\theta \approx 3.0$. In order to show all curves clearly, vertical shifts are made. Note that the points in the tail of the distributions represent the rare occurrences of large clusters which are formed by nodes outside shell $l - 1$.

The branching factor [15] of the network is

$$\tilde{k} = \langle k^2 \rangle / \langle k \rangle - 1,$$

where the averages are calculated for the entire network. For ER network, \tilde{k} can be proved to be equivalent to $\langle k \rangle$. Similarly, we define $\tilde{k}_l \equiv \langle k_l^2 \rangle / \langle k_l \rangle - 1$, where the averages are calculated only for nodes in shell l . Above the diameter, $\tilde{k}_l + 1$ decreases with l for both ER and SF networks (fig. 3b). Thus, at the shells where power law behavior of $P(B_l)$ appears (fig. 2), the nodes have much lower $\tilde{k}_l + 1$ compared with the entire network. The approaching of $\tilde{k}_l + 1$ to 1 (ER network) and 2 (SF network) is consistent with a critical behavior at the boundaries of the network [15].

Next, we study the structural properties of the boundaries. Removing all nodes that are within a distance l (not including shell l) for $l > d$, the network will become fragmented into several clusters (see fig. 1). We denote the size of those clusters as s_l , the number of clusters of size s_l as $n(s_l)$, and the diameter of the cluster as d_l . We find $n(s) \sim s^{-\theta}$, with $\theta \approx 3.0$ (figs. 4a and b). The points in the tails of figs. 4a and b represent the rare appearances of the large clusters. We find similar results for ER and other real networks.

The relation between the sizes of the clusters s_l and their diameters d_l is shown as scatter plots in figs. 5a

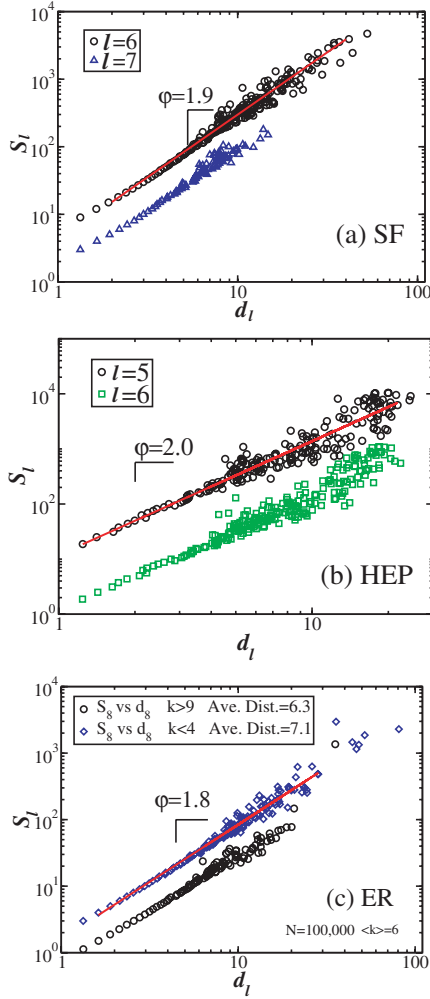


Fig. 5: (Color online) The size of clusters, s_ℓ , shown as scatter plots of the diameters d_ℓ of the clusters for (a) SF network with $N = 10^6$ and $\lambda = 2.5$, (b) HEP citations network for nodes outside shell $\ell - 1$. Vertical shifts of the curves are made for clarity. s_ℓ scales with d_ℓ as $s_\ell \sim d_\ell^\varphi$, with $\varphi \approx 2$. (c) For ER network with $N = 10^5$ and $\langle k \rangle = 6$, s_ℓ as a function of d_ℓ for small degree ($k < 4$) and large degree ($k > 9$) nodes chosen as roots. Here, s_ℓ as a function of d_ℓ is shown for $\ell = 8$. The diameter of the entire network is $d \approx 6.6$. Depending on the degree of the root node, the average distance of all nodes from the root may change. Large degree roots ($k > 9$) have small average distances (≈ 6.3) while small degree roots ($k < 4$) have large average distances (≈ 7.1). However, $s_\ell \sim d_\ell^\varphi$, with $\varphi \approx 2$, can be observed for both small and large degree roots. We ignore the large clusters which appear in the flat regions of fig. 4.

and b, for SF ($\lambda = 2.5$) and HEP citations networks, respectively. In order to show all curves, vertical shifts are made. Figures 5a and b show a power law relation, $s_\ell \sim d_\ell^\varphi$, with $\varphi \approx 2$, suggesting that the clusters at the boundaries are fractals with fractal dimension $d_f = 2$ like percolation clusters at criticality [16,17]. Here, we ignore the non-fractal large clusters which appear in the flat regions of fig. 4. We find that the fractal dimension is $d_f = \varphi \approx 2$ also

for ER, SF with $\lambda = 3.5$ and several other real networks. Root nodes with different degree yield different average distances of the rest of the nodes from the root [18,19]. However, using our definition of boundaries the fractal clusters can be observed for both large and small degree roots (see fig. 5c).

Next we present analytical derivations supporting the above numerical results. We denote the degree distribution of a network as $q(k)$. For infinitely large networks we can neglect loops for $\ell < d$ and approximate the forming of a network as a branching process [20–23]. The probability of reaching a node with k outgoing links through a randomly selected link is $\tilde{q}(k) = (k+1)q(k+1)/\langle k \rangle$. We define $G_0(x) \equiv \sum_{k=0}^{\infty} q(k)x^k$ as the generating function of $q(k)$, $G_1(x) = \sum_{k=0}^{\infty} \tilde{q}(k)x^k = G'_0(x)/\langle k \rangle$ as the generating function of $\tilde{q}(k)$. For ER networks we have $G_0(x) = G_1(x) = e^{\langle k \rangle(x-1)}$ and $\tilde{k} = \langle k \rangle$. The generating function for the number of nodes, B_m , at the shell m is [23]

$$\tilde{G}_m(x) = G_0(G_1(\dots(G_1(x)))) = G_0(G_1^{m-1}(x)), \quad (1)$$

where $G_1(G_1(\dots)) \equiv G_1^{m-1}(x)$ is the result of applying $G_1(x)$, $m-1$ times. $\tilde{P}(B_m)$, which is the probability distribution of B_m , is the coefficient of x^{B_m} in the Taylor expansion of $\tilde{G}_m(x)$.

For shells with large m which is still smaller than d , it is expected [23] that the number of nodes will increase by a factor of k . It is possible to show [21] that $G_1^{m-1}(x)$ converges to a function of the form $f((1-x)\tilde{k}^m)$ for large m ($m \ll d$), where $f(x)$ satisfies the Poincaré functional relation

$$G_1(f(y)) = f(y\tilde{k}), \quad (2)$$

where $y = 1 - x$. The function form of $f(y)$ can be uniquely determined from eq. (2).

It is known [21] that $f(x)$ has an asymptotic functional form, $f(y) = f_\infty + ay^{-\delta} + 0(y^\delta)$, where f_∞ satisfies $G_1(f_\infty) = f_\infty$. It can be shown [22] that f_∞ also gives the probability that a link is not connected to the giant component of the network by one of its ends. Expanding both sides of eq. (2), we obtain

$$G_1(f_\infty) + G'_1(f_\infty)ay^{-\delta} = f_\infty + a\tilde{k}^{-\delta}y^{-\delta} + 0(y^\delta). \quad (3)$$

Since $G_1(f_\infty) = f_\infty$, we have $\delta = -\ln G'_1(f_\infty)/\ln \tilde{k}$.

If $q(1) = 0$ and $q(2) \neq 0$, from $G_1(f_\infty) = f_\infty$, we have $f_\infty = 0$ and $G'_1(f_\infty) = G''_0(0)/\langle k \rangle = 2q(2)/\langle k \rangle$. If $q(2) = q(1) = 0$ (Böttcher case [21]), then $\delta = \infty$, which indicates that $f(y)$ has an exponential singularity. Therefore, networks with minimum degree $k_{\min} \geq 3$ do not have the power law distribution of B_ℓ shown in fig. 2, and therefore have no fractal boundaries.

Applying Tauberian-like theorems [21,24] to $f(y)$, which has a power law behavior for $y \rightarrow \infty$, Dubuc [25] concluded that the Taylor expansion coefficient of $\tilde{G}_m(x)$, $\tilde{P}(B_m)$, behaves as B_m^μ with an exponential cutoff at $B_m^* \sim \tilde{k}^m$, where

$$\mu = \begin{cases} \delta - 1, & q(1) \neq 0 \text{ and } q(2) \neq 0; \\ 2\delta - 1, & q(1) = 0 \text{ and } q(2) \neq 0. \end{cases}$$

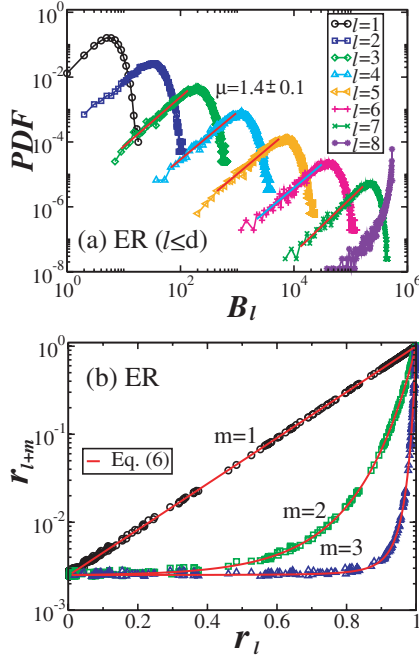


Fig. 6: (Color online) (a) For ER network, the probability distribution function $\tilde{P}(B_\ell)$ of number of nodes B_ℓ in shells $\ell \leq d$. For small values of B_ℓ , $\tilde{P}(B_\ell) \sim B_\ell^\mu$, where μ depends on the $\langle k \rangle$ of the network (eq. (4)). The slopes of the least-square fit represented by the straight lines give $\mu = 1.4 \pm 0.1$, which is in good agreement with the theoretically predicted value $\mu = 1.34$. (b) The fraction of nodes outside shell $\ell + m - 1$, $r_{\ell+m}$, as a function of r_ℓ for ER network, where $r_\ell = 1 - (\sum_{i=1}^{\ell-1} B_i)/N$ is calculated for any possible ℓ . The (red) lines represent the theoretical iteration function (eq. (6)).

Thus the probability distribution function of the number of nodes in the shell m with $m \ll d$ has a power law tail for small values of B_m

$$\tilde{P}(B_m) \sim B_m^\mu. \quad (4)$$

For an ER network, eq. (4) is supported by simulations for $m \leq d$ in fig. 6a. Figure 6a shows for ER network that $\tilde{P}(B_\ell)$ for $\ell < d$ and small values of B_ℓ increase as a power law, $\tilde{P}(B_\ell) \sim B_\ell^\mu$. For ER network, we have $\tilde{k} = \langle k \rangle$, $\mu = \delta - 1$, and $\delta = -\ln G'_1(f_\infty)/\ln \tilde{k}$. Thus $\mu = -\ln(\langle k \rangle f_\infty)/\ln \langle k \rangle - 1$, where f_∞ can be obtained numerically from $f_\infty = e^{\langle k \rangle (f_\infty - 1)}$. In the case of $\langle k \rangle = 6$, $\mu \approx 1.34$, which is close to the result shown in fig. 6a.

The above considerations are correct only for $m < d$, for which the depletion of nodes with large degree in the network is insignificant. In a large network, the shells with $m \gg 1$ behave almost deterministically, and one can apply the mean-field approximation for the number of nodes and links in each shell. Writing down the master equation for the degree distribution in the outer shells, one can obtain a system of ordinary differential equations, which can be solved analytically using the apparatus of generating functions. Using this solution one can show that

$$r_n = G_0(G_1^{n-m}(G_0^{-1}(r_m))), \quad (5)$$

where $r_n = 1 - (\sum_{i=1}^{n-1} B_i)/N$ is the fraction of nodes outside shell $n - 1$. Note that eq. (5) has almost the same structure as eq. (1). It can also be shown that the branching factor of nodes outside shell $n - 1$ is $\tilde{k}(r_n) = uG_0''(u)/G_0'(u)$, where $u = G_0^{-1}(r_n)$.

For ER networks, eq. (5) yields

$$r_{\ell+1} = e^{\langle k \rangle (r_\ell - 1)} = \sum_{k=0}^{\infty} q(k) r_\ell^k, \quad (6)$$

which is valid for all possible ℓ . We test it in fig. 6b for ER network. The relation between $r_{\ell+m}$ and r_ℓ can be obtained by applying eq. (6) m times on r_ℓ . In fig. 6b we show the fraction of nodes outside shell $\ell + m - 1$, $r_{\ell+m}$, as a function of r_ℓ for ER network. Different values of m are tested in the plot.

When $m \ll d$ and $n \gg d$, using the same considerations as we used in eq. (1), one can show that

$$r_n = [a\tilde{k}(1 - r_m)]^{-\mu-1} + r_\infty, \quad (7)$$

where $r_\infty = G_0(f_\infty)$ is the fraction of nodes not belonging to the giant component of the network, a is a constant.

Based on eqs. (4) and (7), expressing r_m and r_n in terms of B_m and B_n , we find that for $m \ll d$ and $n \gg d$, $B_n \sim B_m^{-\mu-1}$. Using $\tilde{P}(B_n)dB_n = \tilde{P}(B_m)dB_m$, we obtain

$$\tilde{P}(B_n) \sim B_n^{-1-\mu/(\mu+1)-1/(\mu+1)} = B_n^{-2}, \quad (8)$$

supporting the numerical findings in fig. 2.

These results are rigorous when \tilde{k} exists and when the minimum degree $k_{\min} \leq 2$. For SF networks with $\lambda < 3$, \tilde{k} diverges for $N \rightarrow \infty$. But for finite N , \tilde{k} still exists. Thus the above results can also be applied to the case of $\lambda < 3$. For both ER and SF networks with $k_{\min} \geq 3$, the power law of $\tilde{P}(B_n)$ with $n \gg d$ cannot be observed, as we indeed confirm by simulations.

Relating our problem to percolation theory, we can explain the simulation results of the probability distribution of cluster size s_ℓ . The cluster size distribution in percolation at some concentration p close to p_c is determined by the formula [15]

$$P_p(s > S) \sim S^{-\tau+1} \exp(-S|p - p_c|^{1/\sigma}). \quad (9)$$

In the case of random networks the percolation threshold is given by $p_c = 1/\tilde{k}$. In the exterior of the shell $n - 1$ ($n \gg d$), we can estimate $|p - p_c| \sim (\tilde{k}(r_n) - 1)/\tilde{k}$, where $\tilde{k}(r_n)$ decreases and reaches the critical percolation value of 1. Near the percolation threshold the nodes outside shell $n - 1$ are split into a number of finite clusters, and if $\tilde{k} > 1$ a giant component. These finite clusters have fractal dimension $d_f = 2$ [16,17]. This theoretical prediction is confirmed in fig. 5.

The cluster size distribution can be estimated by introducing a sharp exponential cutoff at $s = S_n^* \sim |\tilde{k}(r_n) - 1|^{-\frac{1}{\sigma}}$, so that $P_n(s > S) \sim S^{-\tau+1} P(S_n^* > S)$, where $P(S_n^* > S)$ is the probability for a given shell to have

$S_n^* > S$. Since $r_n - r_\infty$ has a smooth power law distribution and $\tilde{k}(r_\infty) < 1$, the probability that $|\tilde{k}(r_n) - 1| < S^{-\sigma} = \varepsilon$ is proportional to ε . Thus $P(S_n^* > S) \sim S^{-\sigma}$ and $P_n(s > S) = S^{-\tau+1-\sigma}$ [26]. Therefore the cluster size distribution follows $n(s) \sim s^{-(\tau+\sigma)} = s^{-\theta}$, thus $\theta = \tau + \sigma$.

For ER networks and SF networks with $\lambda > 4$, $\tau = 2.5$ and $\sigma = 0.5$, the above derivations lead to $n(s) \sim s^{-3}$. For SF networks with $2 < \lambda < 4$, $\tau = (2\lambda - 3)/(\lambda - 2)$ and $\sigma = |\lambda - 3|/(\lambda - 2)$ [16]. Thus, for SF network with $\lambda > 3$, there will be $n(s) \sim s^{-3}$. We conjecture $n(s) \sim s^{-3}$ even for $2 < \lambda < 3$, although in this case $\tilde{k}(r_n)$ does not exist and the above derivations are not valid. Our numerical simulations support these results in fig. 4.

In summary, we find empirically and analytically that the boundaries of a broad class of complex networks including non-fractal networks [9] have fractal features. The probability distribution function of the number of nodes in these shells follows a power law, $\tilde{P}(B_\ell) \sim B_\ell^{-2}$, and the number of clusters of size s_ℓ , $n(s_\ell)$, scales as $n(s_\ell) \sim s_\ell^{-3}$. The clusters at the boundaries are fractals with a fractal dimension $d_f \approx 2$. Our findings can be applied to the study of epidemics. They imply that a strong decay of the epidemic will happen in the boundaries of human network, due to the low degree of nodes.

We thank ONR and Israel Science Foundation for financial support. SVB thanks the Office of the Academic Affairs of Yeshiva University for funding the Yeshiva University high-performance computer cluster and acknowledges the partial support of this research through the Dr. Bernard W. Gamson Computational Science Center at Yeshiva College.

REFERENCES

- [1] ERDŐS P. and RÉNYI A., *Publ. Math.*, **6** (1959) 290; *Publ. Math. Inst. Hung. Acad. Sci.*, **5** (1960) 17.
- [2] BOLLOBÁS B., *Random Graphs* (Academic, London) 1985.
- [3] ALBERT R. and BARABÁSI A.-L., *Rev. Mod. Phys.*, **74** (2002) 47.
- [4] MILGRAM S., *Psychol. Today*, **2** (1967) 60.
- [5] WATTS D. J. and STROGATZ S. H., *Nature (London)*, **393** (1998) 440.
- [6] COHEN R. and HAVLIN S., *Phys. Rev. Lett.*, **90** (2003) 058701.
- [7] DOROGOVTSSEV S. N. and MENDES J. F. F., *Evolution of Networks: from Biological Nets to the Internet and WWW* (Oxford University Press, New York) 2003.
- [8] PASTOR-SATORRAS R. and VESPIGNANI A., *Evolution and Structure of the Internet: Statistical Physics Approach* (Cambridge University Press) 2004.
- [9] SONG C. *et al.*, *Nature (London)*, **433** (2005) 392; *Nat. Phys.*, **2** (2006) 275.
- [10] GOH K. I. *et al.*, *Phys. Rev. Lett.*, **96** (2006) 018701.
- [11] KITSAK M. *et al.*, *Phys. Rev. E*, **75** (2007) 056115.
- [12] Derived from the HEP section of arxiv.org; <http://vlado.fmf.uni-lj.si/pub/networks/data/hep-th/hep-th.htm> (website of Pajek).
- [13] CARMÍ S. *et al.*, *Proc. Natl. Acad. Sci. U.S.A.*, **104** (2007) 11150.
- [14] SHAVITT Y. and SHIR E., *DIMES - Letting the Internet Measure Itself*, <http://www.arxiv.org/abs/cs.NI/0506099>.
- [15] COHEN R. *et al.*, *Phys. Rev. Lett.*, **85** (2000) 4626.
- [16] COHEN R. *et al.*, *Phys. Rev. E*, **66** (2002) 036113; BORNHOLDT S. and SCHUSTER H. G. (Editors), *Handbook of Graphs and Networks* (Wiley-VCH) 2002, Chapt. 4.
- [17] BUNDE A. and HAVLIN S., *Fractals and Disordered System* (Springer) 1996.
- [18] HOLYST J. *et al.*, *Phys. Rev. E*, **72** (2005) 026108.
- [19] DOROGOVTSSEV S. N. *et al.*, *Phys. Rev. E*, **73** (2006) 056122.
- [20] HARRIS T. E., *Ann. Math. Stat.*, **41** (1948) 474; *The Theory of Branching Processes* (Springer-Verlag, Berlin) 1963.
- [21] BINGHAM N. H., *J. Appl. Probab. A*, **25** (1988) 215.
- [22] BRAUNSTEIN L. A. *et al.*, *Int. J. Bifurcat. Chaos*, **17** (2007) 2215; *Phys. Rev. Lett.*, **91** (2003) 168701.
- [23] NEWMAN M. E. J. *et al.*, *Phys. Rev. E*, **64** (2001) 026118.
- [24] WEISS G. H., *Aspects and Applications of the Random Walk* (North Holland Press, Amsterdam) 1994.
- [25] DUBUC S., *Ann. Inst. Fourier*, **21** (1971) 171.
- [26] BARABÁSI A. L. *et al.*, *Phys. Rev. Lett.*, **76** (1996) 2192.